Charging Optimization of Battery Electric Vehicles including Cycle Battery Aging

Annette E. Trippe
Raghavendra Arunachala
Tobias Massier
TUM CREATE
Singapore
annette.trippe@tum-create.edu.sg

Andreas Jossen
Institute for Electrical Energy Storage Technology
Technische Universität München (TUM)
Munich, Germany

Thomas Hamacher
Institute for Renewable and Sustainable Energy Systems
Technische Universität München (TUM)
Munich, Germany

***Abstract*—Controlled charging of battery electric vehicles is one instrument of smart grids in order to intelligently use the electricity load generated by electric vehicles (EVs). However, battery constraints as well as effects of the charging processes on the battery should not be neglected. This work elaborates an EV charging model, which optimizes the charging process while considering cycle battery aging effects. Formulated as a quadratic constraint program, it minimizes total charging cost, consisting of charging electricity cost and battery aging cost. Cycle battery aging tests are conducted and used to analyze and model the battery aging behavior. The optimization model is applied to a sample of EVs in Singapore and four different scenarios are evaluated. The resulting battery aging cost accounts for a substantial share of the total charging cost, i.e., between 52% and 93%. Therefore, an inclusion of battery aging into the intelligent controlling of EV charging is crucial.**

***Index Terms*— Cost optimization, Cycle battery aging, Electric vehicles, Intelligent charging.**

I. Introduction

Looking into smart grids, one aim is to control the charging processes of battery electric vehicles in order to have positive effects on the power system. Therefore, objectives and constraints often refer to the power system and all its components. However, one should consider not only the effects of electric vehicle (EV) charging on the power system, but also the impact on the battery, especially on its aging behavior.

References [1] and [2] are dealing with a multi-objective optimization, where both the energy cost for plug-in hybrid electric vehicles and the battery degradation is minimized. Here, the starting point of charging and the energy amount to recharge is optimized, but not the charging rates. A Pareto-front of several optimal solutions results for each vehicle, which then have to be weighted by energy cost and battery degradation. One battery aging effect is considered, i.e., the growth of the solid electrolyte interphase (SEI) layer. This might be the most important aging effect for the specific battery used in this model, but may not be suitable as the sole effect to reflect battery aging in a general charging optimization model.

In [3] and [4], the influence of different average states of charge (SOCs) on the battery lifetime is compared and analyzed. Various charging strategies including cost optimized charging or battery lifetime optimized charging are investigated and the ratio between charging electricity cost and battery degradation cost is evaluated for the different charging strategies. The model takes into account the SOC as a factor for calendar and cycle battery aging, but not different charging rates.

Our previous work [5] already regarded battery constraints within the charging optimization. However, it considered only the charging processes the battery is capable of, and not how the battery aging is affected during charging.

The purpose of this work is to elaborate a model, which depicts the relationship between charging electricity cost and battery aging cost during a charging process of battery electric vehicles. The developed charging optimization model minimizes electricity cost of the charging process and at the same time aging cost of the vehicle's battery. The cycle battery aging during the charging processes is reflected by a battery aging function, which yields different aging behavior for different charging rates. Cycle battery aging tests are conducted and used to develop a battery aging model. This battery aging model is included in the charging optimization model to minimize total charging cost. As an example case, the optimization is applied to a simulation study of Singapore in order to obtain information on the ratio between charging electricity cost and battery aging cost as well as to allow a deeper understanding of the resulting intelligent charging power profiles.

II. Battery Aging Mechanisms and Cycle tests

In order to consider battery aging within the charging optimization model for electric vehicles, battery aging tests were conducted. After a discussion of the applicable aging effects, the conducted cycle aging tests are described.

This work was financially supported by the Singapore National Research Foundation under its Campus for Research Excellence And Technological Enterprise (CREATE) program.

A. Applicable Battery Aging Effects

Aging mechanisms in lithium ion batteries are complex processes of electrochemical, structural and mechanical degradation that limit the performance and safety of a battery throughout its life, whether it is being used or not. It is mainly characterized by loss of capacity and impedance growth. The most difficult and challenging task is to identify the nature of aging mechanisms as several factors such as environmental conditions, charge and discharge protocols, and rest time influence different aging effects in a battery.

The most common aging effects derived from the usage of a battery in an electric vehicle application are loss of cyclable lithium, surface film formation, electrolyte decomposition, contact loss, active material degradation due to dissolution, structural degradation, delamination of composite material, etc. All these effects can occur simultaneously and in most instances some effects dominate the aging mechanism, depending on the usage of the battery [6], [7].

High ambient temperature reduces the lifetime of the battery by accelerating the aging processes. It increases the rate of parasitic side reactions, leading to irreversible loss of cyclable lithium and causing capacity fade. At high temperatures, the formation of a SEI layer is fostered. The properties of the SEI layer affect its stability at high temperature, leading to dissolution and reformation of the layer. The process of reformation and breakdown of the layer causes impedance rise and capacity fade [8]. High operating voltages have a similar effect as the parasitic side reactions and the accompanying growth of the SEI layer. Furthermore, electrolyte dissolution may occur [9]. High current rates increase the polarization due to the limitation of diffusion as the ionic mass transfer is much slower than the electronic transfer. In addition, the battery temperature increases due to the Joule heating effect. These stress factors lead to faster degradation of the battery.

In a particular application of fast charging, the stress factors as high operating voltage in combination with high current and high temperature occur simultaneously. While in most cycle battery aging studies constant current constant voltage (CCCV) is used, in automotive applications a battery is charged in a constant power (CP) phase followed by a constant voltage (CV) phase. A change in the charging power can significantly influence the amount of time spent in the CP and CV phase respectively. If the charging power is increased, the upper cut-off voltage will be reached at a much earlier time and the battery remains in the CV phase for a longer time. It behaves vice versa for lowering the charging power. Thereby, longer time spent in CV phase reduces the stability of electrolyte and increases the growth of the SEI layer due to high operating voltage [10], [11].

Another important degradation mechanism occurring during fast charging is lithium plating. When the charging current is high, some of the lithium ions are not intercalated into the graphite anode due to the limitation of diffusion, especially at lower temperatures. Under these conditions the non-intercalated ions may be reduced to lithium metal and deposit on the anode surface, decreasing the amount of cyclable lithium ions. If this process continues, the lithium deposition can grow dendrites, causing internal short circuits, which can trigger a thermal runaway in the worst case [7].

B. Battery Testing Procedure

The most prominent chemistries used in automotive applications are lithium nickel cobalt aluminum oxide (NCA), lithium nickel manganese cobalt oxide (NMC), and lithium iron phosphate (LFP) as cathode and graphite as anode material [12]. Cylindrical cells have many safety features such as separator shutdown, current interrupting device, positive temperature coefficient, and pressure vents etc. [13]. The cells chosen for the aging tests are Panasonic 18650 cylindrical cells with a nominal capacity of 2.25 Ah, a nominal voltage of 3.6 V, and a usable energy content of 8.1 Wh. The active material consists of a $Li[NiMnCo]O_2$ cathode, a graphite anode and an organic electrolyte, mainly composed of alkyl carbonate [14]. Hence, the choice of the cell was made based on its chemistry and excellent safety features.

The test regime consisted of characterization tests and cycle aging tests. In the beginning of the test regime, the fresh cells underwent a characterization test to measure the cell capacity and its impedance. After the completion of this test, aging tests were performed. The aging tests were interrupted at regular intervals (50 or 100 cycles) to perform intermediate characterization tests to evaluate the state of health (SOH) of the cells. After the completion of the characterization tests, the aging tests were resumed.

The characterization test consisted of two parts, (1) discharge capacity measurement and (2) hybrid pulse power characterization (HPPC). The cell discharge capacity was measured by first removing the residual capacity, followed by CCCV charging regime at 1 C. A 1 hour pause was provided between successive charge and discharge. The cells were discharged at 1 C to the cut-off voltage in order to measure the discharge capacity. Prior to the beginning of the HPPC test, the cells were completely charged and the HPPC test was conducted as described in [15].

TABLE I. TEST MATRIX FOR CYCLE AGING

Cells	Charge rate	Discharge rate	Characterization tests after
1 - 3	0.2 P (1.70 W)	1 C	100 cycles
4 - 6	0.5 P (4.29 W)	1 C	100 cycles
7 - 9	1 P (8.71 W)	1 C	100 cycles
10 - 12	2 P (17.75 W)	1 C	50 cycles

The aging tests were performed by cycling the cells at different charge rates and a constant discharge rate, as shown in the test matrix in TABLE I. The charging was done in constant power constant voltage (CPCV) mode with the cutoff current 110 mA. The charging power rates were calculated as equivalents of C-rates, i.e., the amount of Ah charged during the CC phase at a specific C-rate equals the amount of Ah charged during the corresponding CP phase. The charging power rates shall be named P-rates in this work, analogue to their equivalent C-rates. The discharge conditions were

constant for all cells, i.e., constant current discharge at 1 C. Three cells were used for each test condition to guard against outliers and manufacturing errors of the cells. The cells were cycled between 3.0 V and 4.2 V. The characterization and aging tests were performed at room temperature (25 ± 2 °C).

III. Methodology of Charging Optimization Model

The charging optimization model consists of three parts. First, data from the battery aging tests is evaluated, analyzed and expressed in functional equations. Second, the controlling of the charging processes is formulated as an optimization problem whereas on the one hand the charging electricity cost and on the other hand the battery aging cost is minimized. Thereby, the equations from the battery aging model are included into the optimization model. Third, the optimization model is applied and solved within a mobility behavior simulation in Singapore.

A. Battery Aging Model

The battery aging model used in this work is based on the aforementioned battery aging tests. In this battery aging model, the physical quantity used to reflect the aging behavior is the energy fade. As it is calculated by multiplying the cell's capacity and average cell voltage, the aging effects causing capacity fade and impedance increase are included. The measurement of the remaining cell discharge capacity during the characterization tests after each 50 or 100 cycles respectively was used together with the cell voltage to determine the energy fade during the cycling. Fig. 1 illustrates the developing of the testing cells' usable energy content for cycling at the four different P-rates. As a common

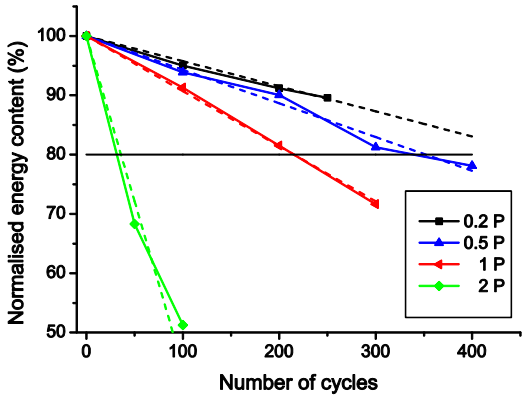

Figure 1. Normalized usable energy content in % and linear approximation (dashed lines) over the course of cycling for four P-rates.

definition, the battery reaches its end of life when the energy content hits 80% of its initial value [16]. The remaining usable energy content as a function of number of cycles shows a nearly linear behavior for the different P-rates and is therefore approximated with a linear slope. The energy fade at each P-rate is expressed by the gradient of the respective linear slope. For 0.2 P, only 250 cycles could be conducted, since for this P-rate one full cycle takes 6.5 hours and the time frame for the aging tests was limited. Since the energy content reached only 90% after 250 cycles, the further decrease of the energy content is extrapolated according to the previous behavior.

A battery aging function is derived from the energy fade data evaluated earlier, i.e., the gradients of the linear slopes describing the developing of the cells' usable energy content. Therefore, the values for energy fade at each P-rate are plotted against the charging power, as depicted in Fig. 2. Analyzing the data points given, the battery aging function could be a polynomial or exponential function. However, instead of hypothesizing on the form of the aging function, we approximate the function piecewise linearly with three secants through the four given data points. The advantage of this approach is a less complex function to be included into the charging optimization model, which in turn leads to a less complex optimization problem. This can be solved with higher computational efficiency and accuracy. This issue will be explained in more detail in the subsequent section.

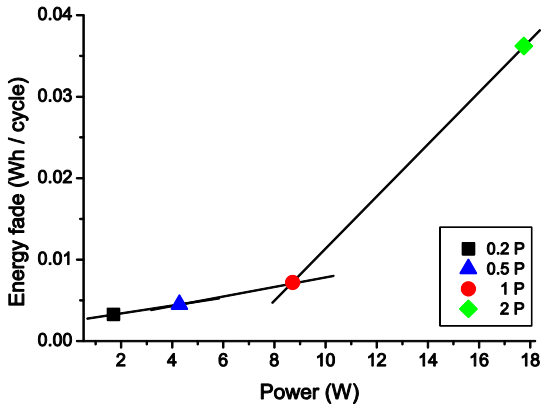

Figure 2. Energy fade in Wh/cycle as a function of charging power and its piecewise linear approximation by three secants.

B. Charging Optimization Model

The objective of the charging optimization model is to minimize the sum of charging electricity cost and battery aging cost. Equation (1) describes the linear objective function of the optimization problem, where charging power P and battery aging cost c_{aging} are the variables to be optimized. The electricity price is reflected by pr and Δt is the length of a time step. n_{park} and t are indices for the number of the parking events of a car and the time respectively.

$$\arg\min_{P,c_{aging}} \sum_{n_{park}} \sum_{t} \left(P\left(n_{park},t\right) \cdot pr\left(t\right) \cdot \Delta t + c_{aging}\left(n_{park},t\right) \right) \qquad (1)$$

The battery aging model is included in the battery aging cost constraint of the optimization problem, as expressed in (2). The constraint contains the three secants approximating the energy fade per cycle as a function of charging power in Fig. 2. The functional equations of the three secants k = 1,2,3 are described by the term $a_k \cdot P\left(n_{park},t\right) + b_k$, where a_k and b_k are the gradient and y-intercept respectively, scaled up to the battery pack size of the respective EV. The scaled energy fade per cycle is divided by the total energy fade over the life cycle,

i.e., the difference of the initial usable energy content $E_{initial}$ and the usable energy content at end of life $E_{EndOfLife}$. Thus, the share of one full cycle in the total energy fade is calculated.

$$c_{aging}\left(n_{park},t\right) \geq \frac{a_k \cdot P\left(n_{park},t\right)+b_k}{E_{initial}\left(n_{park}\right)-E_{EndOfLife}\left(n_{park}\right)} \cdot c_{battery}\left(n_{park}\right) \cdot r_{cha/dis} \cdot \frac{P\left(n_{park},t\right)\cdot \Delta t}{E_{initial}\left(n_{park}\right)} \qquad \forall\, n_{park},t,k \tag{2}$$

The result is multiplied by the battery cost $c_{battery}$ and the aging ratio between charging and discharging $r_{cha/dis}$, in order to obtain the battery aging cost for a full charge at a specific charging power rate. However, since the charging power can be altered within one charging process, the share of each time step (charged at a specific power) in the aging cost of a full charge has to be calculated. This is achieved by multiplying the aging cost of a full charge by the energy share of one time step $P\left(n_{park},t\right)\cdot \Delta t / E_{initial}\left(n_{park}\right)$.

A conservative approach is used to describe the battery aging cost. First, the secants in Fig. 2 lie above the actual aging function – whether polynomial or exponential – and the battery aging cost constraint in (2) is using these secants as lower bound for the battery aging cost. Second, the cycle battery aging tests were conducted without active cooling while cycling. Thus, a temperature rise occurred, especially at higher P-rates, which can lead to faster aging, as explained earlier. However, with an appropriate cooling while charging in an EV application, aging effects might be lower than in the model used in this work. Therefore, the battery aging cost might be lower in reality.

The optimization model contains two more constraints besides the battery aging cost constraint. Equation (3) defines the required energy demand for each parking event and ensures that it is met, where SOC_{start} and SOC_{end} is the state of charge at the beginning and end respectively of a parking event. Equation (4) guarantees, that the charging power P does not exceed the power limit P_{max}, i.e., the power limit of the battery, the charging process, or the charging station, whichever is lower.

$$\sum_t P\left(n_{park},t\right)\cdot \Delta t = E_{initial}\left(n_{park}\right)\cdot \left(SOC_{end}\left(n_{park}\right)-SOC_{start}\left(n_{park}\right)\right) \qquad \forall\, n_{park} \tag{3}$$

$$P\left(n_{park},t\right) \leq P_{\max}\left(n_{park}\right) \qquad \forall\, n_{park},t \tag{4}$$

Since the optimization problem has a linear objective function (1) and quadratic (2) as well as linear constraints (3) and (4), it is a quadratically constrained program (QCP), which is convex and therefore has a unique optimal solution. The advantage of the piecewise linear approximation of the battery aging function, as depicted in Fig. 2, is a quadratic battery aging cost constraint instead of a general nonlinear constraint. Thus, we deal with a QCP instead of a nonlinear program, which can be solved more efficiently. The CPLEX solver [17], called from GAMS [18], is used to solve the QCP.

C. Case Study of Singapore

The charging optimization model is applied to a sample of EVs in Singapore. In order to simulate the driving and parking behavior of electric vehicles, a mobility model specific for Singapore is used, which was elaborated in [19]. A sample of 100 EVs is simulated for one week in time steps of 10 minutes. The simulation creates data including number, length, time, and duration of trips and the according energy consumption, as well as data on parking duration and times.

The mobility model was configured such that EVs charge only when their SOC falls below 60%. If this is the case, it is recharged to a randomly picked SOC up to 97%. This SOC limit is chosen, because it is considered as battery preserving [10], [11]. The EVs are only charged in CP mode in order to avoid the aforementioned damage occurring to the battery during the CV phase. Besides, only a very small amount of energy would be charged to the battery during the long duration of the CV phase. The battery aging model includes full cycles in CPCV charging, but the charging optimization assumes only partial cycles in CP charging. The EVs have batteries of 12 kWh, 16 kWh, 20 kWh, or 24 kWh, which is uniformly distributed among the EVs. The maximum charging power for each parking event of the EVs is set as the minimum of the following three values: the maximum power of the charging station (set to 43.5 kW as in Mode 3 [20]), the maximum power the EV's battery can handle (assumed to be at 2 P charge rate), and the maximum power at which the desired SOC can be reached within the CP phase. In order to calculate the latter, a function was derived from the cycle aging test data, which describes the threshold SOC, where the CP phase transforms into the CV phase, as a function of the charging power. The threshold SOC decreases with rising charging power, as explained earlier. In case the parking duration is too short to reach the desired SOC at the given maximum power limit, the aimed SOC is recalculated to what is possible under the prevailing circumstances.

Further assumptions made for the simulation of charging optimization including cyclic battery aging for a sample of 100 EVs in Singapore are the following: In EV applications, a battery is considered to be at its end of life when the usable energy content has reached 80% of its initial value [16]. The specific battery price is set to 600 USD/kWh [21] in the calculations. The resale value of a depleted battery for second life applications is assumed to amount to 20% of its initial value. The battery cost $c_{battery}$ is calculated by subtracting the resale value of a depleted battery from the price for a new battery. The aging impact of charging is simplifying assumed to be the same as during discharge for different P-rates, setting $r_{cha/dis}$ to 0.5. The electricity price in Singapore was downloaded from the Electricity Market Company website [22] half-hourly for the week from April 7 to 13, 2014. For conversion from SGD to USD, an exchange rate of 1.26 SGD = 1 USD as of April 30, 2014 was used.

IV. Results and Discussion

The aforementioned charging optimization model was applied to a sample of 100 EVs in Singapore, using the assumptions and the mobility model explained before, and so it includes 1043 charging processes which are optimized. It is called the

base scenario subsequently. One EV drives 370 km on average per week [23] and the energy consumption of 100 EVs during this time period is 6,542 kWh. The total cost for 100 EVs amounts to USD 3,387.35, which split into charging electricity cost of USD 667.07 and battery aging cost of USD 2,720.28. The aging cost makes up 80% of the total cost. Fig. 3 (a) shows the total charging power profile of these 100 EVs for two days. The charging power of 100 EVs reaches a maximum of 90.20 kW on Wednesday early evening, while the average charging power per EV is at 0.94 kW. Peaks in the charging power profile tend to occur during valleys in the electricity price which is displayed in Fig. 3 (d).

For comparison, the charging optimization model was executed with omitting the battery aging cost. Thereby, the P-rates can be chosen more freely in order to minimize charging electricity cost. This is achieved by higher power rates compared to the base scenario during time periods with lower electricity price, as pictured in Fig. 3 (b) and (d). This is reflected by the sixfold increase of the maximum total charging power and the elevenfold increase of the average charging power per EV, as shown in TABLE II. Thereby, the charging electricity cost in this scenario could be reduced by 8% to USD 611.73. However, when calculating the battery aging cost for these charging schemes minimizing solely the charging electricity cost, it rises to USD 8,737.13, which is more than three times as high as for the charging optimization including battery aging aspects. For the scenario without battery aging constraints, the battery aging cost accounts for 93% of the total cost. This sums up to USD 9,348.86, which is a substantial increase to the previous scenario. Hence, the advantage of including the battery aging cost into the charging optimization is given.

The aforementioned values for the battery aging cost are very high compared to the charging electricity cost. This can be the case due to the battery aging data used. The cells lasted for 466 to 38 full cycles in the cycle aging tests, depending on the charging power rate lying in a range from 0.2 P to 2 P. For automotive applications, the numbers seem to be insufficient – especially for 2 P charging rates – even though EV manufacturers don't provide information on the number of cycles an EV can endure in fast charging mode. Therefore, a scenario with a longer cycle life of the cells was calculated, assuming 932 full cycles for 0.2 P, i.e., double the cycle life of the testing cells. Within the longer cycle life scenario, charging electricity cost, battery aging cost, as well as total cost decrease, as listed in TABLE II. Now, the battery aging cost's share in the total cost dropped to 68%. The scenario's charging power profile in Fig. 3 (c) resembles the one of the base scenario.

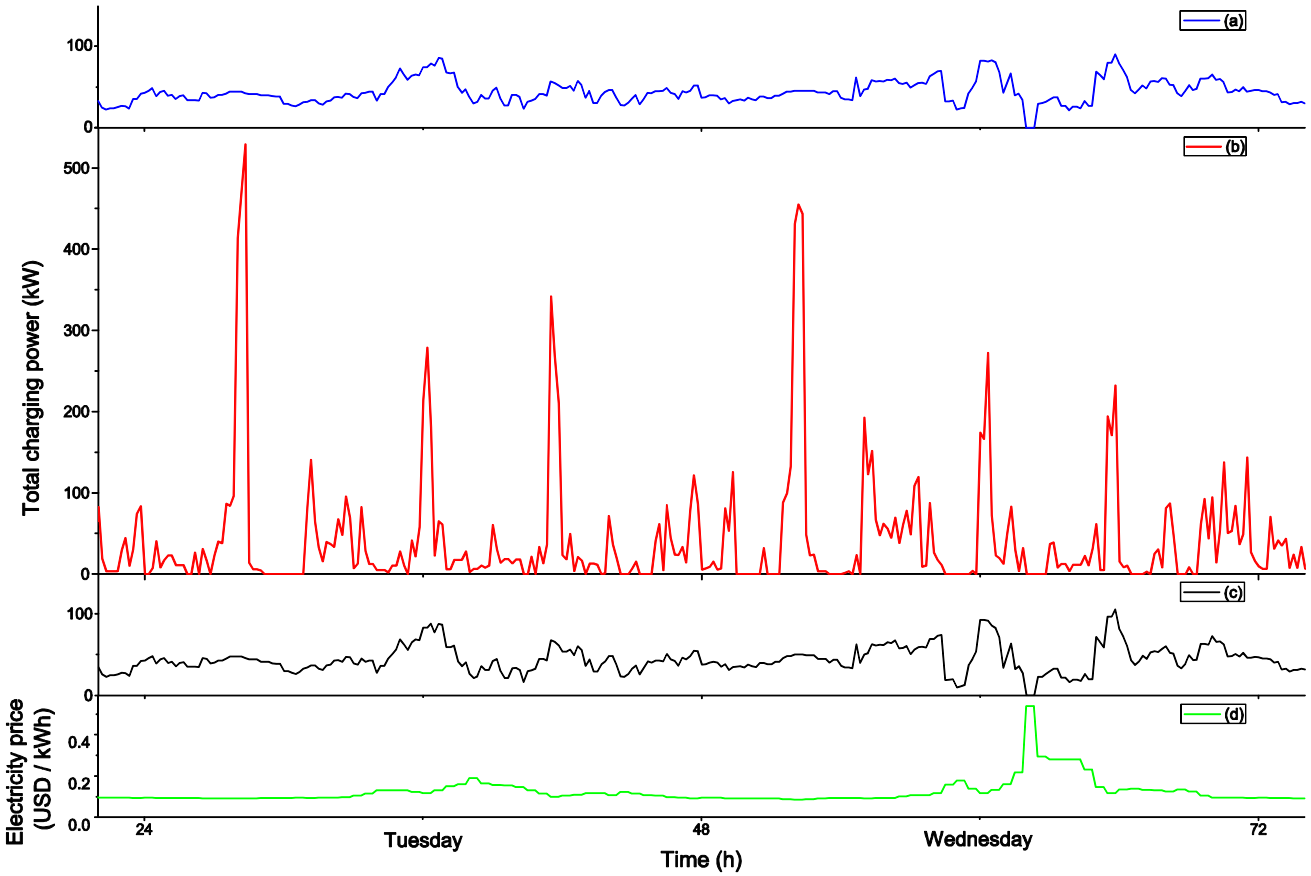

Figure 3. Total charging power profiles in kW for (a) base scenario, (b) scenario without aging constraints, and (c) scenario with longer cycle life as well as (d) electricity price in USD/kWh.

TABLE II. RESULTS OF CHARGING OPTIMIZATION FOR FOUR SCENARIOS

Scenario	Base	w/o aging constraints	Longer cycle life	Future scenario
Total cost (USD)	3,387.35	9,348.86	2,024.30	1,337.41
Charging electricity cost (USD)	667.07	611.73	656.44	645.98
Battery aging cost (USD)	2,720.28	8,737.13	1,367.86	691.43
Max. total charging power (kW)	90.20	555.40	105.13	120.96
Average charging power per EV (kW)	0.94	10.72	0.94	0.94

As decrease in battery cost is expected, a future scenario with a lower specific battery price of 300 USD/kWh [24] and longer cycle life is calculated. In this case, the battery aging cost declines to 52% of the total charging cost.

Regarding the high share of the battery aging cost in all four scenarios, it becomes clear, how important it is to include battery aging factors into an optimization model for the charging processes of EVs. This is also reflected by the battery lifetime, which is three years for the base and six for the longer cycle life and future scenario, but only one year for the scenario without aging constraints with mainly fast charging.

V. CONCLUSION AND OUTLOOK

A charging optimization model for battery electric vehicles including cycle battery aging was elaborated. It minimizes the total cost of charging processes, consisting of charging electricity cost and battery aging cost. The battery aging cost is described by means of data from cycle aging tests conducted in the framework of this work. The charging optimization model was applied to a simulation of 100 EVs in Singapore in order to minimize their total charging cost. The share of the battery aging cost in the total charging cost ranges from 52% to 93%, depending on the scenario. This high share of battery aging cost highlights the significance of the inclusion of battery aging into optimization models for controlled EV charging.

Of course, not only the parameters examined within the conducted scenario analysis have an impact on the results of the model. Other major factors are assumed to be the battery aging data, the resale value of the battery, as well as additional costs, e.g., charging infrastructure cost. The influence of these parameters will be investigated in future work with a profound sensitivity analysis. Furthermore, the battery aging model will be expanded by calendar aging and CV charging effects and the optimization model will be enlarged and configured for a larger sample of EVs as well as a longer time period. Thus, the impact of optimized large scale EV charging on the power system can be evaluated. With these outcomes, the benefits of controlled EV charging for the power system, the effects on the battery, and how both relate to each other, can be examined. Additionally, a profound statement can be made which important aspects in the battery development should be regarded in the future, e.g., higher cycle stability of the battery at high charging rates in order to better facilitate fast charging.

REFERENCES

[1] S. Bashash, S. J. Moura, J. C. Forman, and H. K. Fathy, "Plug-in hybrid electric vehicle charge pattern optimization for energy cost and battery longevity," *J. Power Sources*, vol. 196, no. 1, pp. 541-549, Jan. 2011.

[2] S. Bashash, S. J. Moura, and H. K. Fathy, "On the aggregate grid load imposed by battery health-conscious charging of plug-in hybrid electric vehicles," *J. Power Sources*, vol. 196, no. 20, pp. 8747-8754, Oct. 2011.

[3] B. Lunz, H. Walz, D. U. Sauer, "Optimizing vehicle-to-grid charging strategies using genetic algorithms under the consideration of battery aging," in *2011 IEEE Vehicle Power and Propulsion Conf.*, pp. 1-7.

[4] B. Lunz, Z. Yan, J. B. Gerschler, and D. U. Sauer, "Influence of plug-in hybrid electric vehicle charging strategies on charging and battery degradation costs," *Energy Policy*, vol. 46, pp. 511-519, Jul. 2012.

[5] A. Trippe, T. Massier, and T. Hamacher, "Optimized charging of electric vehicles with regard to battery constraints - case study: Singaporean car park," in *2013 IEEE Energytech*, pp. 1-6.

[6] A. Barré, B. Deguilhem, S. Grolleau, M. Gérard, F. Suard, et al., "A review on lithium-ion battery ageing mechanisms and estimations for automotive applications," *J. Power Sources*, vol. 241, pp. 680-689, 2013.

[7] J. Vetter, P. Novak, M. Wagner, C. Veit, K.-C. Möller, et al., "Ageing mechanisms in lithium-ion batteries," *J. Power Sources*, vol. 147, pp. 269-281, 2005.

[8] D. Abraham, E. Reynolds, P. Schultz, A. Jansen, and D. Dees, "Temperature dependence of capacity and impedance data from fresh and aged high-power lithium-ion cells," *J. of The Electrochemical Society*, vol. 153, pp. A1610-A1616, 2006.

[9] J. Belt, V. Utgikar, and I. Bloom, "Calendar and PHEV cycle life aging of high-energy, lithium-ion cells containing blended spinel and layered-oxide cathodes," *J. Power Sources*, vol. 196, pp. 10213-10221, 2011.

[10] G. Ning, B. Haran, and B. N. Popov, "Capacity fade study of lithium-ion batteries cycled at high discharge rates," *J. Power Sources*, vol. 117, pp. 160-169, 2003.

[11] J. Wang, P. Liu, J. Hicks-Garner, E. Sherman, S. Soukiazian, et al., "Cycle-life model for graphite-$LiFePO_4$ cells," *J. Power Sources*, vol. 196, pp. 3942-3948, 2011.

[12] J. W. Fergus, "Recent developments in cathode materials for lithium ion batteries," *J. Power Sources*, vol. 195, pp. 939-954, 2010.

[13] P. Balakrishnan, R. Ramesh, and T. P. Kumar, "Safety mechanisms in lithium-ion batteries," *J. Power Sources*, vol. 155, pp. 401-414, 2006.

[14] Panasonic, "CGR18650CH lithium ion," data sheet, 2013.

[15] R. Arunachala , K. Makinejad, S. Athlekar, A. Jossen, and J. Garche, "Cycle life characterisation of large format lithium-ion cells," in *Proc. EVS27 International Battery, Hybrid and Fuel Cell Electric Vehicle Symposium,* pp. 1-9.

[16] USABC and DOE National Laboratories, "Electric Vehicle battery test procedures manual," Revision 2, Jan. 1996.

[17] "CPLEX optimizer," 2014. [Online]. Available: http://www-01.ibm.com/software/commerce/optimization/cplex-optimizer/

[18] "GAMS Development Corporation website," 2014. [Online]. Available: http://www.gams.com/

[19] M. Huber, A. Trippe, P. Kuhn, and T. Hamacher, "Effects of large scale EV and PV integration on power supply systems in the context of Singapore," in *Proceedings of 2012 3rd IEEE PES Innovative Smart Grid Technologies Europe (ISGT Europe)*, pp. 1-8.

[20] *Electric vehicle conductive charging system – Part 1: General requirements,* IEC Std. 61851-1, Nov. 2010.

[21] R. Hensley, J. Newman, M. Rogers, and M. Shahinian, "Battery technology charges ahead," McKinsey&Company, 2012.

[22] Energy Market Company (EMC), "Price information," 2014. [Online]. Available: https://www.emcsg.com/marketdata/priceinformation

[23] Land Transport Authority, "Singapore Land Transport Statistics in Brief 2012," 2013. [Online]. Available: http://www.lta.gov.sg

[24] G. Klink, S. Krubasik, T. Rings, and M. Schindler, "E-drive batteries 2025: Überspannung im Batteriemarkt für Elektrofahrzeuge," A.T. Kearney, 2012.